Dynamics of helical strips

Alain Goriely[1,2,*] and Patrick Shipman[2]
[1]*Program in Applied Mathematics, Building No. 89, University of Arizona, Tucson, Arizona 85721*
[2]*Department of Mathematics, Building No. 89, University of Arizona, Tucson, Arizona 85721*
(Received 4 October 1999)

The dynamics of inertial elastic helical thin rods with noncircular cross sections and arbitrary intrinsic curvature, torsion, and twist is studied. The classical Kirchhoff equations are used together with a perturbation scheme at the level of the director basis, and the dispersion relation for helical strips is derived and analyzed. It is shown that all naturally straight helical strips are unstable whereas free-standing helices are always stable. There exists a one-parameter family of stationary helical solutions depending on the ratio of curvature to torsion. A bifurcation analysis with respect to this parameter is performed, and bifurcation curves in the space of elastic parameters are identified. The different modes of instabilities are analyzed.

PACS number(s): 45.05.+x, 46.25.−y

I. INTRODUCTION

The analysis of helical structures plays an important role in the study of various types of chemical and biological fibers such as DNA, bilipid layers, and macrofibers [1–7]. Recently, there has been a great deal of attention paid to the stability of different configurations of elastic helical strips [8]. Most analyses are limited to comparisons of elastic energies (in the context of both linear and nonlinear elasticity) [9,10]. This approach reveals that binormal helices (such as the strips shown in Fig. 1) are more likely to be stable. Another approach consists in studying the dynamical stability of stationary solutions within the framework of the Kirchhoff equation for thin rods. This has been done for helical rods with circular cross sections in [11] and shown to be of prime importance in the analysis of buckling and coiling [12]. When the cross section of the rod loses its isotropy (that is, when one considers elastic strips), the type of instability found in twisted rods strongly depends on the anisotropy of the cross sections [13,14] and two different regimes can be found depending on the flatness of the cross section.

This paper considers the dynamics of helical inextensible elastic rods of various lengths, cross sectional shapes, and material properties. If a rod obeys the laws of elasticity and has a cross sectional width much smaller than its length, it is referred to as a *filament* or, in the case of noncircular cross sections, as a *strip*. Consider such an elastic strip and shape it as a helix such that it will hold by itself (with proper end forces and moments). This helical strip can be stable or unstable under small perturbations. The problem is to determine the stability properties of such configurations and provide some information on the wavelengths associated with the instability. The analysis performed here provides also the vibration modes associated with stable configurations.

II. THE KIRCHHOFF EQUATIONS

The evolution of filaments and strips is governed by the Kirchhoff model, where forces and moments are averaged over local cross sections of the rod attached to its central axis [15]. The central axis is represented by a space curve $\mathbf{R}(s,t):\mathbb{R}^2\rightarrow\mathbb{R}^3$ parametrized by arc length s and time t. A right-handed orthonormal basis is established at each point of $\mathbf{R}(s,t)$ by the well-known Frenet frame ($\mathbf{n}$, $\mathbf{b}$, $\mathbf{t}$) consisting of the tangent vector $\mathbf{t}$, the normal vector $\mathbf{n}$, which is the unit vector in the direction of $\partial\mathbf{t}/\partial s$, and the binormal vector $\mathbf{b}=\mathbf{t}\times\mathbf{n}$. The turning rate with respect to s of the plane orthonormal to the curve—that is, the plane defined by ($\mathbf{n}$, $\mathbf{b}$)—is related to the Frenet curvature $\kappa(s,t)=|\partial\mathbf{t}(s,t)/\partial s|$, and the Frenet torsion $|\tau(s,t)|=|\partial\mathbf{b}(s,t)/\partial s|$ is related to the rate of turning with respect to s of the plane tangent to $\mathbf{R}(s,t)$—that is, the plane defined by ($\mathbf{n}$, $\mathbf{t}$). The curvature and torsion $\kappa(s,t)$ and $\tau(s,t)$ determine the space curve through the Frenet-Serret equations. For example, if these values are both nonzero and constant with respect to s, then $\mathbf{R}(s,t)$ is a helix.

The Frenet frame and its associated definitions of curvature and torsion are derived from the space curve itself. For a physical filament, however, it is advantageous to have a local basis that corresponds to some characteristic of the filament's material properties. Here we are interested in helical filaments of constant asymmetrical (not circular) cross sections, referred to as *strips*, and, using a generalized local basis for the space curve, we set one of the vectors normal to the

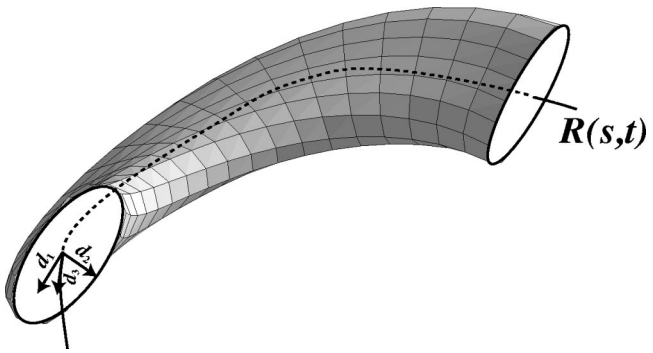

FIG. 1. A typical strip $\mathbf{R}(s,t)$ together with its coordinate orthonormal triad $(\mathbf{d}_1,\mathbf{d}_2,\mathbf{d}_3)$. The vectors $\mathbf{d}_1,\mathbf{d}_2$ are chosen along the direction of greatest and lowest bending stiffness. The vector $\mathbf{d}_3$ is tangent to the curve.

*Electronic address: goriely@math.arizona.edu

 © 2000 The American Physical Society

curve to correspond to the direction of the filament's greatest bending stiffness. Also, we allow for intrinsic curvature and twist—i.e., the curvature and twist of the filament in its natural, unstressed state. Stationary helical solutions for the Kirchhoff equations were described in [14]. The aim of this paper is to study the stability of helical strips using an arc-length-preserving perturbation scheme first developed in [16]. This follows work in [11] on the stability of helical rods of circular cross sections and in [14] on straight strips.

Together with the space curve $\mathbf{R}(s,t)$ we choose a smooth unit vector field $\mathbf{d}_2(s,t)$ orthogonal to the tangent vector of the curve and along the direction of the cross section's lowest bending stiffness. The vector $\mathbf{d}_2(s,t)$ is part of a local coordinate triad $(\mathbf{d}_1,\mathbf{d}_2,\mathbf{d}_3)$ defined at each (s,t). If we consider a very flat strip (think of a belt), the vector $\mathbf{d}_3$ is the tangent vector along the center axis and the vector $\mathbf{d}_1$ is chosen in the direction joining the center axis to the edge of the strip (in the ''flattest'' direction) as can be seen on Fig. 1. Denoting differentiation with respect to s and t by $(\,)'$ and $(\dot{\ })$, respectively, and setting $\mathbf{d}_3=\mathbf{R}'(s,t)$, we choose $\mathbf{d}_1$ to be the unit vector field such that $\mathbf{d}_1=\mathbf{d}_2\times\mathbf{d}_3$, and then $(\mathbf{d}_1,\mathbf{d}_2,\mathbf{d}_3)$ is, for all (s,t), a local right-handed orthonormal basis. It is related to the Frenet frame $(\mathbf{n},\mathbf{b},\mathbf{t})$ by the angle ζ between the two bases and the relation

$$(\mathbf{d}_1\quad\mathbf{d}_2\quad\mathbf{d}_3)=(\mathbf{n}\quad\mathbf{b}\quad\mathbf{t})\begin{pmatrix}\cos\zeta & -\sin\zeta & 0\\ \sin\zeta & \cos\zeta & 0\\ 0 & 0 & 1\end{pmatrix}. \tag{1}$$

The local triad $(\mathbf{d}_1,\mathbf{d}_2,\mathbf{d}_3)$ evolves in space and time as

$$(\mathbf{d}_1'\quad\mathbf{d}_2'\quad\mathbf{d}_3')=(\mathbf{d}_1\quad\mathbf{d}_2\quad\mathbf{d}_3)K, \tag{2}$$

$$(\dot{\mathbf{d}}_1\quad\dot{\mathbf{d}}_2\quad\dot{\mathbf{d}}_3)=(\mathbf{d}_1\quad\mathbf{d}_2\quad\mathbf{d}_3)W, \tag{3}$$

where $\mathbf{K}$ and $\mathbf{W}$ are the antisymmetric matrices

$$\mathbf{K}=\begin{pmatrix}0 & -\kappa_3 & \kappa_2\\ \kappa_3 & 0 & -\kappa_1\\ -\kappa_2 & \kappa_1 & 0\end{pmatrix},$$

$$\mathbf{W}=\begin{pmatrix}0 & -\omega_3 & \omega_2\\ \omega_3 & 0 & -\omega_1\\ -\omega_2 & \omega_1 & 0\end{pmatrix}. \tag{4}$$

The vectors $\boldsymbol{\kappa}=\Sigma_{i=1}^{3}\kappa_i\mathbf{d}_i$, $\boldsymbol{\omega}=\Sigma_{i=1}^{3}\omega_i\mathbf{d}_i$, formed from components of $\mathbf{K}$ and $\mathbf{W}$, are respectively defined as the twist and spin vectors.

The twist vector is related to the angle ζ and the Frenet curvature κ and torsion τ as

$$(\kappa_1,\kappa_2,\kappa_3)=\left(\kappa\sin\zeta,\kappa\cos\zeta,\tau+\frac{\partial\zeta}{\partial s}\right). \tag{5}$$

One may think of τ, κ, and $\partial\zeta/\partial s$ as variations on the filament's twist: τ measures the nonplanarity of $\mathbf{R}(s,t)$; κ and $\partial\zeta/\partial s$ are both properties of the ribbon defined by the curve $\mathbf{R}(s,t)$ along with the orthogonal field $\mathbf{d}_2(s,t)$. An intrinsic twist vector $\boldsymbol{\kappa}^{(u)}=(\kappa_1^{(u)},\kappa_2^{(u)},\kappa_3^{(u)})$ is designed to correspond to $(\kappa_1,\kappa_2,\kappa_3)$ so that we have an intrinsic curvature $\kappa^{(u)}=\sqrt{(\kappa_1^{(u)})^2+(\kappa_2^{(u)})^2}$, and an intrinsic twist $\kappa_3^{(u)}$. As in Eq. (5),

$$\kappa_1^{(u)}=\kappa^{(u)}\sin\zeta\quad\text{and}\quad\kappa_2^{(u)}=\kappa^{(u)}\cos\zeta. \tag{6}$$

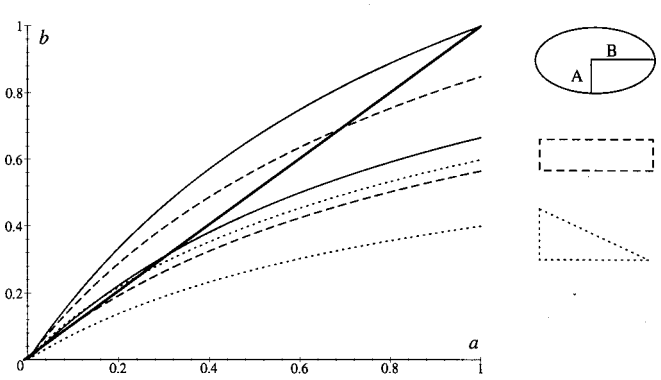

FIG. 2. The domains covered in the (a,b) plane by various cross section shapes with $0\leqslant\sigma\leqslant 1/2$ are enclosed in black lines (solid=ellipses, dash=rectangles, dot=right triangles). The line $b=a$ plays an important role in the stability analysis of binormal helices.

Let I_1 and I_2 be the principal moments of inertia of the cross section in the directions of $\mathbf{d}_1$ and $\mathbf{d}_2$, respectively, with $I_1\geqslant I_2$. That is, $\mathbf{d}_1$ and $\mathbf{d}_2$ are chosen to be the directions of greatest and lowest bending stiffnesses, respectively. Then, $a=I_2/I_1$ is a value $0<a\leqslant 1$ that measures the bending asymmetry of the filament's cross sections. The value 1 is reached in the dynamically symmetric case where the moments of inertia are identical; the scaled radius of circular cross sections is then equal to 2. A constant b, called the *scaled torsional stiffness*, roughly measures the change in volume in the rod as it is stretched. The lower the value of b, the less the volume changes. Within the framework of linear elasticity theory [17–19] it is possible to compute a and b for a given cross section shape. For instance, elliptic cross sections with semiaxes A and B $(A<B)$ have

$$a=\frac{A^2}{B^2},\quad b=\frac{1}{1+\sigma}\,\frac{2a}{1+a}, \tag{7}$$

where σ is the Poisson ratio. The scaled semiaxes are, respectively, $2\sqrt{a}$ and 2. Other values of a and b for various shapes are represented on Fig. 2. With a force vector $\mathbf{F}=F_1\mathbf{d}_1+F_2\mathbf{d}_2+F_3\mathbf{d}_3$ and moment vector M, the scaled dynamical Kirchhoff equations stated in the local basis are [14]

$$\mathbf{F}''=\ddot{\mathbf{d}}_3, \tag{8a}$$

$$\mathbf{M}'+\mathbf{d}_3\times\mathbf{F}=a\,\mathbf{d}_1\times\ddot{\mathbf{d}}_1+\mathbf{d}_2\times\ddot{\mathbf{d}}_2, \tag{8b}$$

$$\mathbf{M}=(\kappa_1-\kappa_1^{(u)})\mathbf{d}_1+a(\kappa_2-\kappa_2^{(u)})\mathbf{d}_2+b(\kappa_3-\kappa_3^{(u)})\mathbf{d}_3. \tag{8c}$$

The static (without time dependence) form of these equations is

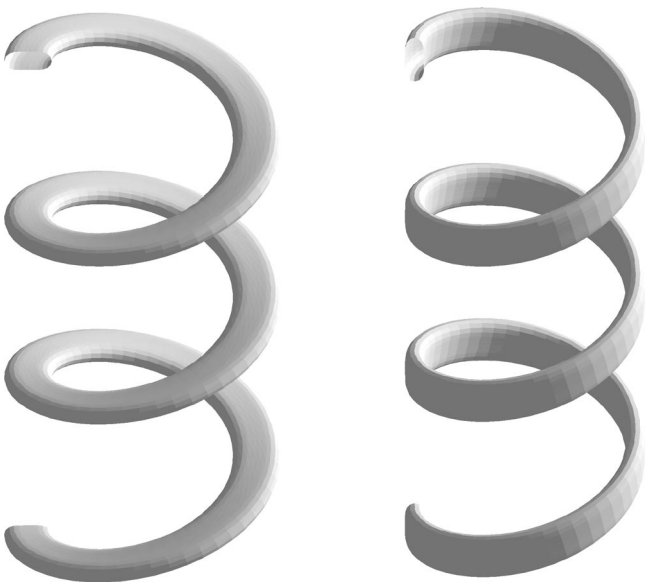

FIG. 3. Normal and binormal helices.

$$\mathbf{F}' = \mathbf{0}, \tag{9a}$$

$$\mathbf{M}' + \mathbf{d}_3 \times \mathbf{F} = \mathbf{0}, \tag{9b}$$

$$\mathbf{M} = (\kappa_1 - \kappa_1^{(u)})\mathbf{d}_1 + a(\kappa_2 - \kappa_2^{(u)})\mathbf{d}_2 + b(\kappa_3 - \kappa_3^{(u)})\mathbf{d}_3. \tag{9c}$$

Helical and circular solutions to these equations are those with constant Frenet curvature and torsion (we consider here true helices for which both curvature and torsion are different from zero). The only such solutions are those with the angle between the director basis and the Frenet frame an integer multiple of $\pi/2$ [14]. That is, $\zeta = n\pi/2$, where n is an integer. These solutions are such that $\partial\zeta/\partial s = 0$ and are called Frenet helices since the principal axes do not rotate with respect to the Frenet frame. Moreover, for a helix to be a solution we need

$$\kappa\tau^{(u)} = \kappa^{(u)}\tau. \tag{10}$$

That is, helical strips are stationary solutions of the Kirchhoff equations only if they are twistless and the ratio of curvature to torsion equals the ratio of intrinsic curvature to intrinsic torsion. There are two types of solutions depending on the parity of n. For even n, $\mathbf{d}_2$ lies along the binormal vector $\mathbf{b}$, which is then the direction of lowest bending stiffness. Such helical solutions, namely,

$$\boldsymbol{\kappa} = \kappa\mathbf{d}_2 + \tau\mathbf{d}_3, \tag{11a}$$

$$\mathbf{F} = (b-a)\tau(\boldsymbol{\kappa} - \boldsymbol{\kappa}^{(u)}), \tag{11b}$$

are referred to as *binormal helices*. For odd n, $\mathbf{d}_2$ lies along the normal vector n. These solutions, namely,

$$\boldsymbol{\kappa} = \kappa\mathbf{d}_1 + \tau\mathbf{d}_3, \tag{12a}$$

$$\mathbf{F} = (b-1)\tau(\boldsymbol{\kappa} - \boldsymbol{\kappa}^{(u)}), \tag{12b}$$

are referred to as *normal helices* (see Fig. 3).

III. PERTURBATION EXPANSION

To study the stability of these solutions, a perturbation scheme was developed for the Kirchhoff equations in [20,21]. A perturbation is performed by a near-identity rotation matrix $\mathbf{B}$ that maps the unperturbed local basis onto the perturbed one:

$$(\mathbf{d}_1 \quad \mathbf{d}_2 \quad \mathbf{d}_3) = (\mathbf{d}_1^{(0)} \quad \mathbf{d}_2^{(0)} \quad \mathbf{d}_3^{(0)})\mathbf{B}, \tag{13a}$$

$$\mathbf{d} = \mathbf{d}^{(0)} + \epsilon\mathbf{d}^{(1)} + \epsilon^2\mathbf{d}^{(2)} + \ldots, \tag{13b}$$

and requiring to each order in ϵ that the orthonormality condition $\mathbf{d}_i \cdot \mathbf{d}_j = \delta_{ij}$ is satisfied. Expanding $\mathbf{B}$ as a power series in ϵ, we obtain

$$\mathbf{B} = \mathbf{1} + \varepsilon\mathbf{A}^{(1)} + \varepsilon^2(\mathbf{A}^{(2)} + \mathbf{S}^2) + \varepsilon^3(\mathbf{A}^{(3)} + \mathbf{S}^{(3)}) + \ldots, \tag{14}$$

where $\mathbf{1}$ is the identity matrix, and the symmetric matrices $\mathbf{S}^{(k)}$ depend solely on the general antisymmetric matrices $\mathbf{A}^{(1)}$ to $\mathbf{A}^{(k-1)}$, where the $\mathbf{A}^{(j)}$'s are

$$\mathbf{A}^{(j)} = \begin{pmatrix} 0 & -\alpha_3^{(j)} & \alpha_2^{(j)} \\ \alpha_3^{(j)} & 0 & -\alpha_1^{(j)} \\ -\alpha_2^{(j)} & \alpha_1^{(j)} & 0 \end{pmatrix}. \tag{15}$$

Given the vector $\boldsymbol{\alpha} = (\alpha_1, \alpha_2, \alpha_3)$, where $\alpha_i = \alpha_i^{(1)}$, one can reconstruct the perturbed rod by integrating the tangent vector as

$$\mathbf{R}(s,t) = \int \mathbf{d}_3(s,t)\,ds = \int [\mathbf{d}_3^{(0)} + \epsilon(\alpha_2\mathbf{d}_1^{(0)} - \alpha_1\mathbf{d}_2^{(0)})]ds + O(\epsilon^2). \tag{16}$$

Expressions for the elements of the twist $\boldsymbol{\kappa}$ and spin $\boldsymbol{\omega}$ vectors in terms of the perturbed variables are obtained using Eqs. (2) and (13a) which combine to give

$$\frac{\partial}{\partial s}[(\mathbf{d}_1^{(0)} \quad \mathbf{d}_2^{(0)} \quad \mathbf{d}_3^{(0)})\mathbf{B}] = (\mathbf{d}_1^{(0)} \quad \mathbf{d}_2^{(0)} \quad \mathbf{d}_3^{(0)})\mathbf{B}\mathbf{K}. \tag{17}$$

This, in turn, is equivalent to

$$(\mathbf{d}_1^{(0)} \quad \mathbf{d}_2^{(0)} \quad \mathbf{d}_3^{(0)})\left(\mathbf{K}^{(0)}\mathbf{B} - \mathbf{B}\mathbf{K} + \frac{\partial\mathbf{B}}{\partial s}\right) = \mathbf{0}. \tag{18}$$

Since the matrix $\mathbf{B}$ is orthogonal and the basis vectors are independent, we have

$$\mathbf{K} = \mathbf{B}^T\left(\mathbf{K}^{(0)}\mathbf{B} + \frac{\partial\mathbf{B}}{\partial s}\right). \tag{19}$$

The spin vector components are expressed analogously. For a given unperturbed state, the Kirchhoff equations may now be written in terms of the six variables of the vector

$$\mathbf{X}^{(k)} = (F_1^{(k)} \quad F_2^{(k)} \quad F_3^{(k)} \quad \alpha_1^{(k)} \quad \alpha_2^{(k)} \quad \alpha_3^{(k)})^T. \tag{20}$$

IV. CONSTRUCTION OF THE PERTURBED HELICAL STRIPS

It was previously noted that, given the vector $\boldsymbol{\alpha}=(\alpha_1,\alpha_2,\alpha_3)$, we can construct the perturbed strip by the integration (16). To actually perform this integration we need the vector $\boldsymbol{\alpha}$ and the generalized frame $\mathbf{d}^{(0)}=(\mathbf{d}_1^{(0)},\mathbf{d}_2^{(0)},\mathbf{d}_3^{(0)})$ of the unperturbed helix.

The vector $\mathbf{d}^{(0)}$ is found by the relation (1) and the Frenet frame of a helical curve, which is as follows:

$$\begin{pmatrix}\mathbf{n}\\ \mathbf{b}\\ \mathbf{t}\end{pmatrix}=\begin{pmatrix}(0,-\cos(\delta s),-\sin(\delta s))\\ (-R\delta,-P\delta\sin(\delta s),P\delta\cos(\delta s))\\ (P\delta,-R\delta\sin(\delta s),R\delta\cos(\delta s))\end{pmatrix}, \tag{21}$$

where R is the radius of the cylinder about which the helix may be wrapped, $P\pi$ is the period of the helix, and $\delta=\pm\sqrt{1/(P^2+R^2)}$. The positive root in this last expression defines a right-handed helix, and the negative root defines a left-handed helix. For a binormal helix, with $\zeta=n\pi/2$ for even n, Eq. (1) gives

$$\mathbf{d}^{(0)}=\begin{pmatrix}\mathbf{n}\\ \mathbf{b}\\ \mathbf{t}\end{pmatrix}. \tag{22}$$

Hence, Eq. (16) becomes

$$\mathbf{R}(s,t)=\int\left\{\begin{pmatrix}P\delta\\ -R\delta\sin(\delta s)\\ R\delta\cos(\delta s)\end{pmatrix}+\boldsymbol{\epsilon}\left[\alpha_2\begin{pmatrix}0\\ -\cos(\delta s)\\ -\sin(\delta s)\end{pmatrix}-\alpha_1\begin{pmatrix}-R\delta\\ -P\delta\sin(\delta s)\\ P\delta\cos(\delta s)\end{pmatrix}\right]\right\}ds+O(\boldsymbol{\epsilon}^2). \tag{23}$$

For the normal helix $\zeta=n\pi/2$, n odd, so Eq. (1) gives

$$\mathbf{d}^{(0)}=\begin{pmatrix}\mathbf{b}\\ -\mathbf{n}\\ \mathbf{t}\end{pmatrix}, \tag{24}$$

and Eq. (16) becomes

$$\mathbf{R}(s,t)=\int\left\{\begin{pmatrix}P\delta\\ -R\delta\sin(\delta s)\\ R\delta\cos(\delta s)\end{pmatrix}+\boldsymbol{\epsilon}\left[\alpha_2\begin{pmatrix}-R\delta\\ -P\delta\sin(\delta s)\\ P\delta\cos(\delta s)\end{pmatrix}-\alpha_1\begin{pmatrix}0\\ \cos(\delta s)\\ \sin(\delta s)\end{pmatrix}\right]\right\}ds+O(\boldsymbol{\epsilon}^2). \tag{25}$$

The vector $\boldsymbol{\alpha}$ is found by finding the vector solutions (20) corresponding to unstable modes, as described below.

V. STABILITY ANALYSIS

The linearization of the Kirchhoff equations around the stationary helical solutions allows for a stability analysis. The unperturbed variables $\mathbf{F}^{(0)}$ and $\boldsymbol{\kappa}^{(0)}$ are taken to be the static helical solutions, Eq. (11) for a study of the binormal helix and Eq. (12) for a study of the normal helix. The $\boldsymbol{\epsilon}^0$-order part of the spin vector expansion, $\boldsymbol{\omega}^{(0)}$, is set to 0, and the expansions for tension, twist, and spin vectors, truncated to first order, are substituted into the system. The result, in matrix form, is

$$\mathbf{L}\mathbf{X}^{(1)}=\mathbf{0}, \tag{26}$$

where $\mathbf{L}$ for the binormal helix is the following second-order linear operator:

$$L=\begin{pmatrix}L_A & L_B\\ L_C & L_D\end{pmatrix}, \tag{27}$$

where

$$L_A=\begin{pmatrix}\frac{\partial^2}{\partial s^2}-\kappa^2-\tau^2 & -2\tau\frac{\partial}{\partial s} & 2\kappa\frac{\partial}{\partial s}\\ 2\tau\frac{\partial}{\partial s} & \frac{\partial^2}{\partial s^2}-\tau^2 & \kappa\tau\\ -2\kappa\frac{\partial}{\partial s} & \kappa\tau & \frac{\partial^2}{\partial s^2}-\kappa^2\end{pmatrix}, \tag{28}$$

$$L_B=\begin{pmatrix}2(b-a)(\kappa^2+\tau^3)\frac{\partial}{\partial s} & (b-a)\tau^2\left(\frac{\partial^2}{\partial s^2}\kappa^2-\tau^2\right)-\frac{\partial^2}{\partial t^2} & (b-a)\tau\kappa(\tau^2+\kappa^2-\partial^2\partial s^2)\\ (b-a)\tau^2\left(\kappa^2+\tau^2-\frac{\partial^2}{\partial s^2}\right)+\frac{\partial^2}{\partial t^2} & 2(b-a)\tau^3\frac{\partial}{\partial s} & -2(b-a)\kappa\tau^2\frac{\partial}{\partial s}\\ (b-a)\tau\kappa\left(\frac{\partial^2}{\partial s^2}-\tau^2-\kappa^2\right) & -2(b-a)\kappa\tau^2\frac{\partial}{\partial s} & 2(b-a)\kappa^2\tau\frac{\partial}{\partial s}\end{pmatrix}, \tag{29}$$

$$L_C=\begin{pmatrix}0 & -1 & 0\\ 1 & 0 & 0\\ 0 & 0 & 0\end{pmatrix}, \tag{30}$$

$$L_D=\begin{pmatrix}(b-a)(\tau^2-\kappa^2)-a\kappa\kappa_2^u-b\tau\kappa_3^u+\dfrac{\partial^2}{\partial s^2}-\dfrac{\partial^2}{\partial t^2} & (b-a-1)\tau\dfrac{\partial}{\partial s}-b\kappa_3^u\dfrac{\partial}{\partial s} & (b-a+1)\kappa\dfrac{\partial}{\partial s}+a\kappa_2^u\dfrac{\partial}{\partial s}\\ (1+a-b)\tau\dfrac{\partial}{\partial s}+b\kappa_3^u\dfrac{\partial}{\partial s} & (b-1)\tau^2-b\tau\kappa_3^u+a\left(\dfrac{\partial^2}{\partial s^2}-\dfrac{\partial^2}{\partial t^2}\right) & (1-b)\kappa\tau+\kappa_3^u\\ (a-b-1)\kappa\dfrac{\partial}{\partial s}-\alpha\kappa_2^u\dfrac{\partial}{\partial s} & (1-a)\kappa\tau+a\kappa_2^u\tau & b\dfrac{\partial^2}{\partial s^2}(a-1)\kappa^2-a\kappa\kappa_2^u-(1+a)\dfrac{\partial^2}{\partial t^2}\end{pmatrix}. \tag{31}$$

We now look for the fundamental solutions of Eq. (26), expressed as

$$\mathbf{X}^{(1)}=A\mathbf{u}e^{\tau(\sigma t+ins)}, \tag{32}$$

where A is a constant complex amplitude, $\mathbf{u}$ is a constant vector with a given norm, σ is a complex constant, and n is a real constant. The substitution of Eq. (32) into Eq. (26) yields

$$\mathbf{M}\mathbf{u}=\mathbf{0}. \tag{33}$$

The matrix $\mathbf{M}$ for the binormal helix is

$$M=\begin{pmatrix}M_A & M_B\\ M_C & M_D\end{pmatrix}, \tag{34}$$

where

$$M_A=\begin{pmatrix}-(1+n^2)\tau^2-\kappa^2 & -2in\tau^2 & 2in\kappa\tau\\ 2i\tau^2n & -(1+n^2)\tau^2 & \kappa\tau\\ -2in\kappa\tau & \kappa\tau & -\kappa^2-\tau^2n^2\end{pmatrix}, \tag{35}$$

$$M_B=\begin{pmatrix}2i\tau n(F_2+\tau F_3) & -\kappa\tau F_2-(\tau^2n^2+\tau^2)F_3-\tau^2\sigma^2 & (\tau^2n^2+\kappa^2)F_2+\kappa\tau F_3\\ 2\kappa\tau F_2+[(1+n^2)\tau^2-\kappa^2]F_3+\tau^2\sigma^2 & 2in\tau^2F_3 & -2in\tau^2F_2\\ -2\kappa\tau F_3-[(n^2-1)\tau^2+\kappa^2]F_2 & -2in\kappa\tau F_3 & 2in\kappa\tau F_2\end{pmatrix}, \tag{36}$$

$$M_C=\begin{pmatrix}0 & -1 & 0\\ 1 & 0 & 0\\ 0 & 0 & 0\end{pmatrix}, \tag{37}$$

$$M_D=\begin{pmatrix}(b-a)(\tau^2-\kappa^2)-\tau^2(n^2+\sigma^2)-a\kappa\kappa_2^{(u)}-b\tau\kappa_3^{(u)} & in\tau^2(b-a-1)-ibn\tau\kappa_3^{(u)} & in\kappa\tau(b-a+1)+ian\tau\kappa_2^{(u)}\\ in\tau^2(1+a-b)+ibn\tau\kappa_3^{(u)} & \tau^2(b-1-an^2-a\sigma^2)-b\tau\kappa_3^{(u)} & (1-b)\kappa\tau+b\kappa\kappa_3^{(u)}\\ in\kappa\tau(a-b-1)-ian\tau\kappa_2^{(u)} & (1-a)\kappa\tau+a\kappa_2^{(u)}\tau & (a-1)\kappa^2-bn^2\tau^2-(1+a)\tau^2\sigma^2-a\kappa\kappa_2^{(u)}\end{pmatrix}, \tag{38}$$

and the expressions $F_2=(b-a)\tau(\kappa-\kappa_2^{(u)})$ and $F_3=(b-a)\tau(\tau-\kappa_3^{(u)})$ are the components of the force vector $\mathbf{F}$. The matrix $\mathbf{M}$ for the normal helix has a similar form (with different coefficients) and will not be given explicitly here. There are nontrivial solutions for $\mathbf{u}$ only if $\det(M)=0$. This leads to the *dispersion relation*

$$\det(M)=\Delta(n,\sigma^2,a,b,\tau,\kappa,\zeta_i,\kappa_i^{(u)},\kappa_3^{(u)})=0, \tag{39}$$

where $i=1$ for the normal helix (in this case $\zeta_1=\pi/2$ and $\kappa_1^{(u)}=\kappa^{(u)}$, $\kappa_2^{(u)}=0$) and $i=2$ for the binormal helix ($\zeta_2=0$ and $\kappa_1^{(u)}=0$, $\kappa_2^{(u)}=\kappa^{(u)}$) due to relations (6). If the dis-

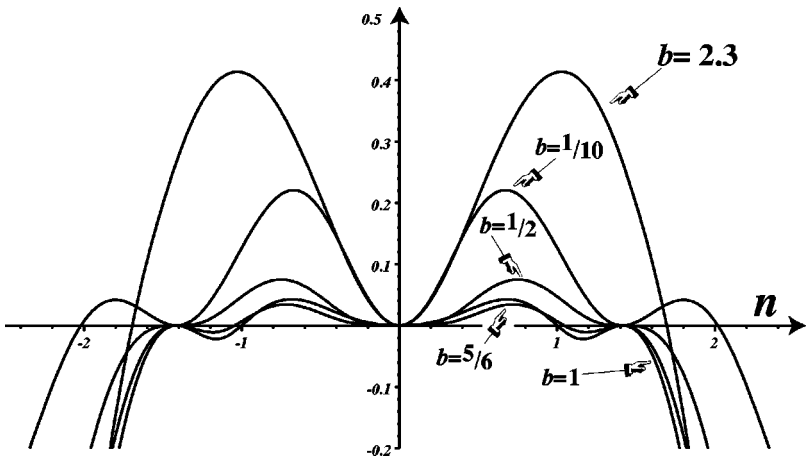

FIG. 4. Naturally straight binormal helix: $\varsigma(n)$ with $\kappa=1=\tau$, $a=1/2$, and $b=1/10$, 1/2, 5/6, 1, and 2.3.

persion relation allows for modes that grow exponentially in time—that is, modes with $\mathrm{Re}(\sigma)>0$—then the helical strip is unstable.

The dispersion relations corresponding to the binormal and the normal helices are examined for the existence of these unstable modes. We first study the stability of the naturally straight helices—those with $\boldsymbol{\kappa}^{(u)}$ set to $\mathbf{0}$—and then the stability of the free-standing helices—those with $\boldsymbol{\kappa}^{(u)}$ set to $\boldsymbol{\kappa}$. The basic procedure is the following. We solve Eq. (39) for σ^2 as a function of n and the parameters a, b, τ, and κ, and thus obtain three solutions $\sigma_1^2(n)$, $\sigma_2^2(n)$, and $\sigma_3^2(n)$. We are interested in the real parts of these solutions. For the binormal helix, whether $\boldsymbol{\kappa}=\mathbf{0}$ or $\boldsymbol{\kappa}=\boldsymbol{\kappa}^{(u)}$, we find that the solution σ_2 is purely imaginary regardless of the values of the intrinsic curvature and twist, and $\mathrm{Re}[\sigma_3^2(n)]\leqslant 0$ for all n, so these solutions contribute no unstable modes. The situation for the normal helix is similar; the solution $\mathrm{Re}(\sigma_3^2)$ is nonpositive for all n and although the solution $\sigma_2^2(n)$ may have a real part (in the case $\boldsymbol{\kappa}^{(u)}=\mathbf{0}$), this part is always nonpositive. Hence, we only consider the solution $\varsigma(n)=\mathrm{Re}[\sigma_1^2(n)]$.

VI. THE NATURALLY STRAIGHT HELICES

We first consider naturally straight helices, that is, helices with no intrinsic curvature or torsion ($\boldsymbol{\kappa}^{(u)}=\mathbf{0}$). The neutral modes—the values of n such that $\mathrm{Re}(\sigma)=0$—are found by substituting $\sigma^2=0$ into the dispersion relation (39) and solving for n. For both the normal and binormal helices we find neutral modes of the form

$$n_1=0, \tag{40a}$$

$$\pm n_2=\pm\frac{\sqrt{\tau^2+\kappa^2}}{\tau}, \tag{40b}$$

$$\pm n_3=\pm\frac{\sqrt{2}}{2}\frac{\psi+\sqrt{\chi}}{ba\tau}, \tag{40c}$$

$$\pm n_4=\pm\frac{\sqrt{2}}{2}\frac{\psi-\sqrt{\chi}}{ba\tau}, \tag{40d}$$

where ψ and χ are rather complicated functions of $b-a$, τ, and κ. The neutral modes n_1 and n_2 are independent of $b-a$; hence we organize a discussion of unstable modes by considering values of $b-a$ since the stability changes occur as the roots n_3 and n_4 change position relative to the root n_2.

A. The naturally straight binormal helix

Taking $\zeta=\zeta_2=0$ and $\kappa_2^{(u)}=0$ in the dispersion relation we find the solution $\varsigma(n)$ associated with the naturally straight binormal helix. Various examples of this solution, with constant κ, τ, and a, and varying b, are shown in Fig. 4. The graphs indicate positive concavity at $n=0$ for most values of $b-a$. To show that this is indeed the case, we locally expand the dispersion relation around $n=0$ and find

$$\varsigma=\epsilon^2(\alpha+\sqrt{\beta})\frac{\kappa^2+\tau^2}{\gamma}n_1^2+\epsilon^3\varsigma^{(3)}+\ \ldots\ , \tag{41}$$

where α, β, and γ are all functions of the parameters κ, τ, a, and b. For small ϵ, ς behaves approximately like $(\alpha+\sqrt{\beta})[(\kappa^2+\tau^2)/\gamma]n_1^2$. Since γ is always positive, the sign of the lowest order term in the expansion of $\varsigma(n)$ about (0,0) depends on $\alpha+\sqrt{\beta}$. For $b\leqslant a$ and $\frac{1}{3}[(4\tau^2+\kappa^2)/\tau^2]a<b$, $\beta-\alpha^2>0$, so $\alpha+\sqrt{\beta}>0$. Thus, $\varsigma(n)$ has positive concavity at (0,0) for these values of the parameters. For the range $a<b<\frac{1}{3}[(4\tau^2+\kappa^2)/\tau^2]a$, ς has negative concavity at (0,0). However, for these values, both modes n_3 and n_4 appear as roots of $\varsigma(n)$, and in this range $\varsigma(n)$ has the form shown in Fig. 5. Hence, we conclude that a naturally straight binormal helix is always unstable. Depending on the values of a and b, there are two different types of unstable modes. In the range $b\leqslant a$ and $\frac{1}{3}[(4\tau^2+\kappa^2)/\tau^2]a<b$ the instability is a long wave instability (all modes close to $n=0$ are unstable), and the deformation takes place on long wavelengths. For $a<b<\frac{1}{3}[(4\tau^2+\kappa^2)/\tau^2]a$, there is an unstable band of modes centered around a nonzero wave number n_c. This Hopf-like instability occurs at finite wavelength and results in the superposition of two helical modes: the stationary solution and the unstable solution with wave number n_c.

To construct the solution, we find the fundamental solutions corresponding to the fastest-growing mode n_c—that is, the mode that corresponds to a peak in the solutions $\varsigma(n)$.

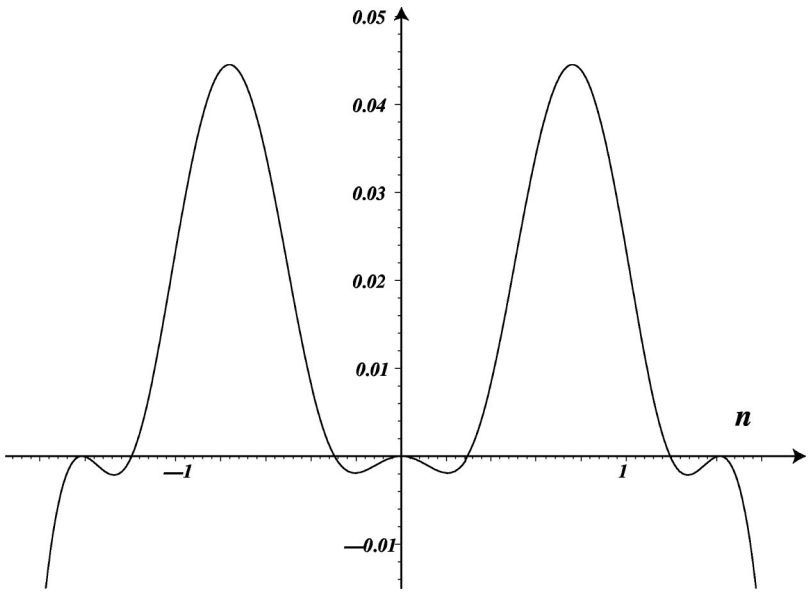

FIG. 5. Naturally straight binormal helix: $\varsigma(n)$ with $\kappa=1=\tau$, $a=1/2$, and $b=2/3$.

For example, for the binormal helix with properties as listed in Fig. 5 ($\kappa=1=\tau, a=\frac{1}{2}, b=\frac{2}{3}$), the fastest-growing modes are those at $n\approx 0.7704$. The corresponding null vector of Eq. (34) is

$$\mathbf{u}\approx\begin{pmatrix} -0.392i \\ 0.427 \\ -0.294 \\ 1.769 \\ 0.402 \\ -1.443 \end{pmatrix}. \tag{42}$$

Similarly, $n_c=-0.7704$ yields the complex conjugate of this solution vector $\overline{\mathbf{u}}$. The corresponding solution is then

$$A\mathbf{u}e^{[\varsigma(0.7704)t+0.7704is]}+\overline{A}\overline{\mathbf{u}}e^{[\varsigma(0.7704)t-0.7704is]}, \tag{43}$$

and the last three components of this vector form $\boldsymbol{\alpha}$.

Examples of perturbed binormal naturally straight helical strips follow in Fig. 6. In all cases, we use $A=1$, $R=2=P$, and $\delta=\frac{1}{2}$. Two periods are shown. For different values of b, two unstable wavelengths can be excited. For instance, for $a=\frac{1}{2}$ and $b=\frac{1}{10}$, the dispersion relation (Fig. 4) shows two maxima around $n_c=\pm 0.6685$ and $n_c=\pm 1.797$. The reconstructed unstable binormal helix is shown in Fig. 7.

B. The naturally straight normal helix

Taking $\zeta=\zeta_1=\pi/2$ and $\kappa_1^{(u)}=0$ in the dispersion relation we find the solution $\varsigma(n)$ associated with the naturally straight normal helix. Typical graphs of this solution are shown in Fig. 8 for fixed κ, τ, and a, and varying b. As indicated there, there is a band of unstable modes around $n=0$, and this band grows as the value $b-a$ increases. Setting $n=0$ in $\det(M)$ and solving for σ^2, we get the three roots 0, 0, and $[(1-a^2)(\tau^2\kappa^2+\tau^4)+(1-a)(\kappa^4+\tau^2\kappa^2+\kappa^2)+(\tau^2+\kappa^2)^2+\kappa^2]/[\tau^2(\kappa^2+\tau^2+1)(a+1)]$. The first two roots

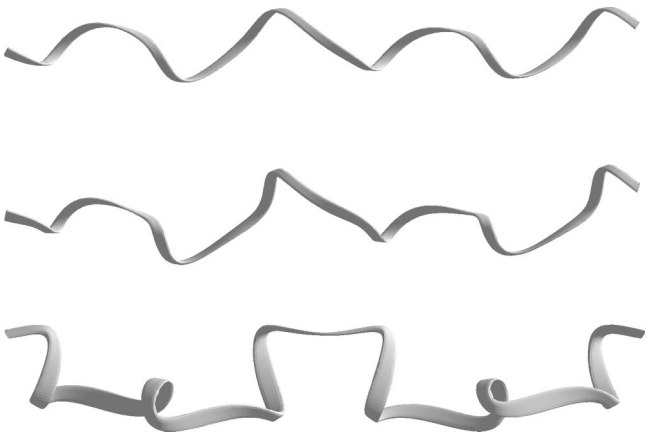

FIG. 6. Binormal helix, $a=1/2$, $b=2/3$, $\tau=1=\kappa$, $\kappa_2^{(0)}=0=\kappa_3^{(0)}$, perturbed modes: $n_c=\pm 0.7704$, $\epsilon=0.1$, 0.2, and 0.5.

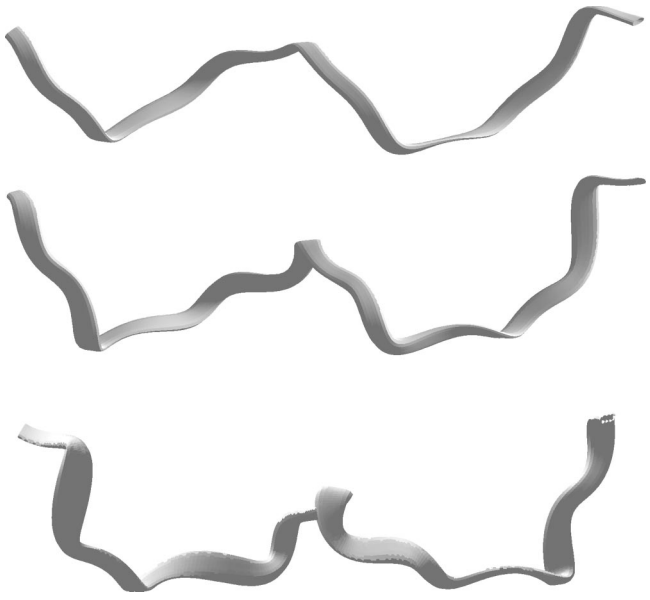

FIG. 7. Binormal helix, $a=1/2$, $b=1/10$, $\tau=1=\kappa$, $\kappa_2^{(0)}=0=\kappa_3^{(0)}$, perturbed modes: $n_c=\pm 0.6685$, ± 1.797, $\epsilon=0.1$, 0.2, and 0.3.

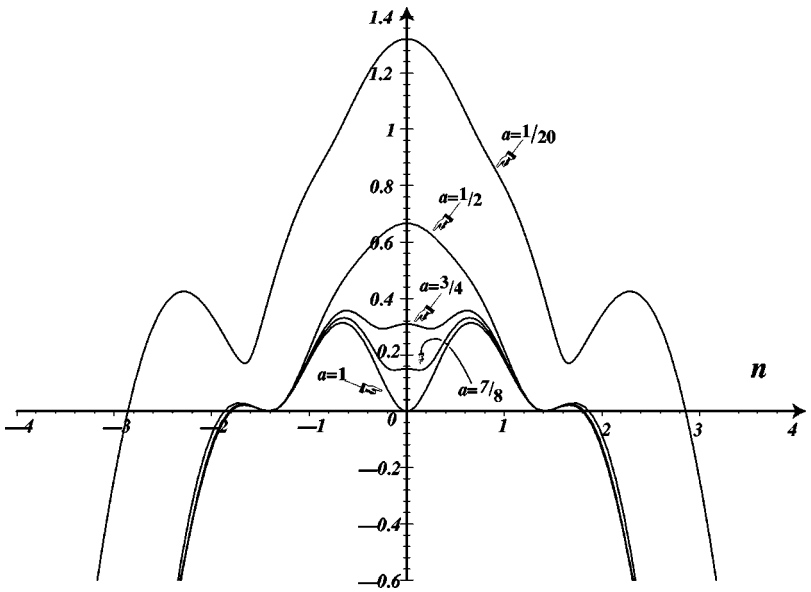

FIG. 8. The solution $\varsigma(n)$ for normal helices with $\kappa=1=\tau$, $b=3/4$, and $a=1/20$, 1/2, 3/4, 7/8, and 1.

appear in the solutions σ_2^2 and σ_3^2, and the last appears in the solution $\varsigma(n)=\sigma_3^2$. Since $a\leqslant 1$ the last root is always positive. Hence there is always a band of unstable modes about $n=0$ in the solution $\varsigma(n)$. We conclude that, as for the naturally straight binormal helix, the naturally straight normal helix is always unstable.

VII. THE FREE-STANDING HELICES

For the case $\boldsymbol{\kappa}^{(u)}=\boldsymbol{\kappa}$ we have only two neutral modes, which are

$$n_1=0, \tag{44a}$$

$$\pm n_2=\pm\frac{\sqrt{\tau^2+\kappa^2}}{\tau}. \tag{44b}$$

These neutral modes all appear as roots of the solution $\varsigma(n)$. A local perturbation analysis around the points $(n,s)=(0,0),(\pm\sqrt{\tau^2+\kappa^2}/\tau,0)$ as performed for the naturally straight binormal helix shows that the curve $\varsigma(n)$ always has negative concavity around these points. Hence, there are no unstable modes, and we conclude that the free-standing helices are always (linearly) stable.

VIII. HELICES THAT ARE NEITHER NATURALLY STRAIGHT NOR FREE STANDING

Let $r=\tau/\kappa$ be the aspect ratio of a helix; $r>1$ are long helices whereas $r<1$ are ''fat'' helices. Stationary helical solutions are such that $\kappa\tau^{(u)}=\tau\kappa^{(u)}$. Let R be the ratio

$$R=\frac{\tau^{(u)}}{\tau}=\frac{\kappa^{(u)}}{\kappa}. \tag{45}$$

For a given intrinsic torsion and curvature the one-parameter family of helices defined by R corresponds to similar helices of different size (helices with constant ratio of torsion to curvature). The natural size is defined as the size of the helix with $R=1$. The radius of such a helix is $\rho^{(u)}=\kappa^{(u)}/[(\kappa^{(u)})^2+(\tau^{(u)})^2]$. For $R\neq 1$ the radius of the helix is $\rho=R\rho^{(u)}$. Hence R describes the relative size of similar helices. For $R>1$ the helices are smaller than the natural size, and bigger for $R<1$. In the preceding sections we studied the case $R=0$ (naturally straight helices) and $R=1$ (free-standing helices). We now consider values of R different from 0 and 1. If we start at $R=1$, the helix is stable. As we vary this parameter, the helix might become unstable. The question is to locate the bifurcation point R_c for given a and b and to describe the instability.

Again, we need only consider the real part of one solution to the dispersion relation since the other two solutions always have nonpositive real parts, and we call this real part of a solution $\varsigma(n)$. For example, a graph of $\varsigma(n)$ corresponding to the normal helix with fixed values of κ, τ, a, and b, and varying R is shown in Fig. 9. Note that, for example, if $R=\frac{1}{2}$, $b=\frac{3}{2}$, and $a<\frac{3}{4}$, then there are no unstable modes for the normal helix; a helix must not be free standing to be stable. An analysis of the neutral modes $\pm n_3$ and $\pm n_4$ given in Eq. (44) allows for the finding of the values of the parameters that characterize stable forms. For $r=1$ in the normal case we have the situation indicated by Fig. 10, where stable regions are those in which $\pm n_3$ and $\pm n_4$ are not neutral modes, and the solution $\varsigma(n)$ is similar to the $R=1$ case of Fig. 9. The stability of a stationary helix (normal or binormal) depends on r, R, a, and b. For both helices, the picture is similar to the one in Fig. 9. We set $c=1$ for the normal helix and $c=a$ for the binormal helix. We find that for $b<c$, the helix is stable only for $1\leqslant R\leqslant R'$, and for $b>c$ the helix is stable only for $R'\leqslant R\leqslant 1$, where the values of R' are given by the positions of the different roots. We have considered that all modes can be excited (short, middle, and long wavelength instabilities).

Most helical strips are such that $b<1$ (see Fig. 2); hence, all normal helices behave the same way. They are stable as long as $1\leqslant R<R'$; when the size is such that $R>R'$ a short wavelength instability develops (the unstable modes $n_c>1$); and smaller helices ($R<1$) are all unstable with a long wavelength instability.

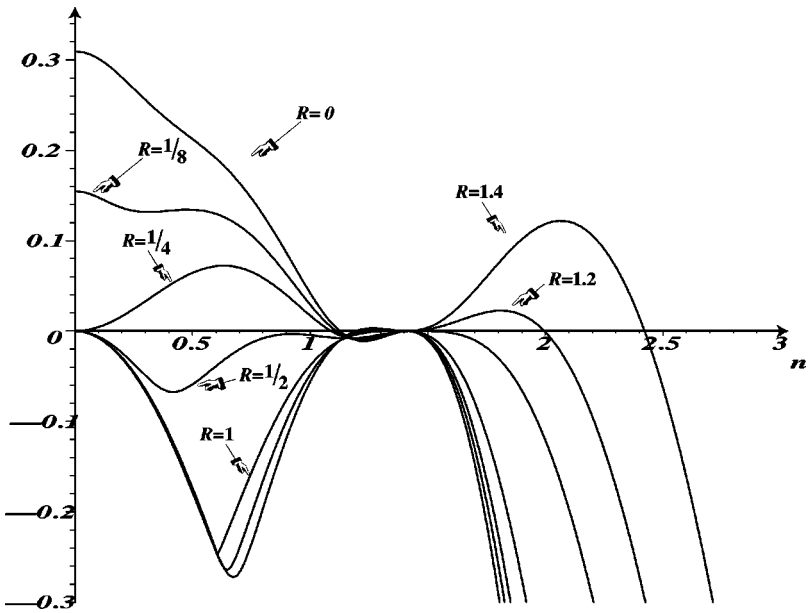

FIG. 9. Normal helix: $\varsigma(n)$ with $\kappa=1=\tau$, $a=3/4$, and $b=3/2$ and varying R.

The situation for binormal helices is slightly different. For $b<a$, the helix is stable only for $1\leqslant R\leqslant R'$, and for $b>a$ the helix is stable only for $R'\leqslant R\leqslant 1$, So, depending on the cross section anisotropy, binormal helices can become unstable. Indeed, for a given b and flat cross sections (such that $a<b$) small helices can be stable (for $R'<R<1$), whereas helices with thick cross sections ($a<b$) behave like normal helices.

IX. INSTABILITY OF CIRCULAR STRIPS

In order to show how boundary conditions can stabilize instabilities, we study the case of elastic rings with anisotropic cross sections. This case is of particular interest in the theory of DNA rings Ref. [22]. In the case of elastic rings, $\tau=0$, hence we do not scale the mode n with τ and we let $R=\kappa^{(u)}/\kappa$. The filament is periodic (of period $2\pi/\kappa$) and with periodic boundary conditions on the force and curvature vectors as well as the position vector. This restricts considerably the type of instabilities since modes with long wavelengths (with $n/\kappa<1$) cannot become unstable and only discrete modes can be unstable (with $n/\kappa>1$ and integer). Due to this fact, small binormal rings (with $R\leqslant 1$) are always stable and large rings of increasing size first become unstable when $n/\kappa=2$. The mode $n/\kappa=m$ becomes unstable for $R>R_m$, where

$$R_m=\frac{2a-(1+b)+\sqrt{(b-1)^2+4bm^2}}{2a}>1. \qquad (46)$$

Surprisingly, normal rings can become unstable when either $R<1$ or $R>1$. Indeed, the mth mode becomes unstable whenever $0\leqslant R<R_m^{(1)}$ or $R>R_m^{(2)}>1$ with

$$R_m^{(1)}=1-\tfrac{1}{2}(a+b)-\tfrac{1}{2}\sqrt{(b-a)^2+4m^2ab}, \qquad (47)$$

$$R_m^{(2)}=1-\tfrac{1}{2}(a+b)+\tfrac{1}{2}\sqrt{(b-a)^2+4m^2ab}. \qquad (48)$$

Note that $R_m^{(1)}>0$ only if $a<(1-b)/[(m^2-1)b+1]$. Hence, the cross section has to be sufficiently flat for small normal rings to become unstable. In the particular case of circular cross sections one finds that $R_m=R_m^{(2)}$ and $R_m^{(1)}<0$ and we recover the solution given in Ref. [23].

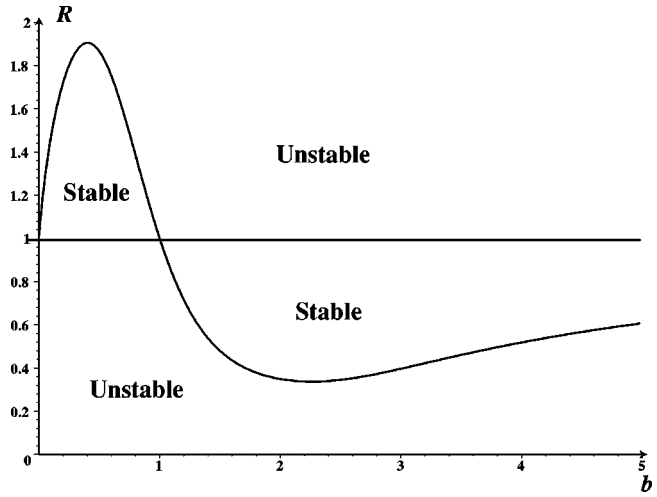

FIG. 10. Bifurcation curves (R-b plane) for the normal helix with $\kappa=1=\tau$, $a=3/4$. The different regions indicate the zones of stability and instability.

X. CONCLUSIONS

In this paper, we have studied the stability of normal and binormal helices. The first conclusion is that all (infinitely long) naturally straight strips shaped as helices are unstable. This might seem contradictory to one's intuition. Indeed, if one plays with a belt (or a very flat strip of paper), it is easy to create a binormal helical strip by twisting one end. In the same way, it is next to impossible to shape a strip as a normal helix. However, if one considers flat enough strips ($a<b$), one sees on Fig. 4 that the unstable mode appears between 0 and $\sqrt{2}$. These are long wavelength modes only ($\sqrt{2}$ is the mode associated with the helical repeat, hence n

$<\sqrt{2}$ correspond to wavelengths longer than the helical repeats). We conclude that a *finite helical binormal strip* clamped at both ends is stable if its cross section is flat enough. In the case of a normal helix, there always exist unstable modes with $n>\sqrt{2}$ and these modes become more important as the cross sections become flatter (see Fig. 8). Therefore, we conclude that normal helices with flat cross sections are always unstable even for finite strips.

Our second conclusion is that free-standing helices are always stable. This is not surprising as these helices correspond to minima of the elastic energy and we do not expect them to become dynamically unstable. The analysis performed here can be used in this case to provide all the vibration modes of the stable helix; these are the (imaginary) time exponents associated with the modes (40). Depending on the type of constraints imposed, one can easily obtained the corresponding descriptions of the vibrations. In particular, the spring constants of Hooke's law can be obtained together with higher order corrections and coupling to other modes.

The effect of size on the stability of helices was also studied. Depending on the ratio R that measures the size of a stationary helix with respect to the corresponding free-standing helix and the aspect ratio r, we showed that small normal helices are always unstable. Moreover, depending on the anisotropy of the cross sections, small binormal helices can be stable (for flat cross sections) or unstable (thick cross sections). The analysis of stability becomes quite intricate in general, and a detailed analysis of the roots of the dispersion relation has to be performed.

Finally, we studied circular strips. Whereas only large (with $R>1$) binormal circular strips may be unstable, small normal circular strips with flat cross sections may also have instabilities.

ACKNOWLEDGMENTS

One of the authors (A.G.) would like to thank Michael Tabor for many fruitful discussions. This work was supported by the NSF under Grant No. DMS-9972063, by NATO-CRG 97/037 and the Alfred P. Sloan Foundation (A.G.).

[1] N. H. Mendelson, Proc. Natl. Acad. Sci. USA **75**, 2472 (1978).
[2] C. J. Benham, Biopolymers **18**, 609 (1979).
[3] J. H. White and W. R. Bauer, J. Mol. Biol. **189**, 329 (1986).
[4] Y. Yang, I. Tobias, and W. K. Olson, J. Chem. Phys. **98**, 1673 (1993).
[5] J. H. Fuhrhop and W. Helfrich, Chem. Rev. **93**, 1565 (1993).
[6] F. Jülicher, Phys. Rev. E **49**, 2429 (1994).
[7] B. D. Coleman, E. H. Dill, and D. Swigon, Arch. Ration. Mech. Anal. **129**, 147 (1995).
[8] R. L. Ricca, J. Phys. A **28**, 2335 (1995).
[9] W. Helfrich, J. Chem. Phys. **85**, 1085 (1986).
[10] W. Helfrich, Langmuir **7**, 567 (1991).
[11] A. Goriely and M. Tabor, Proc. R. Soc. London, Ser. A **453**, 2583 (1997).
[12] A. Goriely and M. Tabor, Proc. R. Soc. London, Ser. A **454**, 3183 (1998).
[13] G. H. M. van der Heijden and J. M. Thompson, Physica D **112**, 201 (1998).
[14] A. Goriely, M. Nizette, and M. Tabor (unpublished).
[15] B. D. Coleman, E. H. Dill, M. Lembo, Z. Lu, and I. Tobias, Arch. Ration. Mech. Anal. **121**, 339 (1993).
[16] A. Goriely and M. Tabor, Phys. Rev. Lett. **77**, 3537 (1996).
[17] L. D. Landau and E. M. Lifshitz, *Theory of Elasticity* (Pergamon, Oxford, 1959).
[18] A. E. H. Love, *A Treatise on the Mathematical Theory of Elasticity* (Cambridge University Press, Cambridge, 1892).
[19] I. S. Sokolnikoff, *Mathematical Theory of Elasticity* (McGraw-Hill, New York, 1956).
[20] A. Goriely and M. Tabor, Physica D **105**, 20 (1997).
[21] A. Goriely and M. Tabor, Physica D **105**, 45 (1997).
[22] W. Han, S. M. Lindsay, M. Daklic, and R. E. Harrington, Nature (London) **386**, 563 (1997).
[23] Z. Haijun and O.-Y. Zhong-can, J. Chem. Phys. **110**, 1247 (1999).